Journal of
Materials Chemistry A

Materials for energy and sustainability

Accepted Manuscript

This article can be cited before page numbers have been issued, to do this please use: S. Wang, S. Li, L. Nie and Y. Chen, *J. Mater. Chem. A*, 2025, DOI: 10.1039/D5TA02030A.

ROYAL SOCIETY OF CHEMISTRY

rsc.li/materials-a

View Article Online
DOI: 10.1039/D5TA02030A

Reasonable active site design for promoting water dissociation and carbon monoxide activation in low temperature water-gas shift reaction

Shikun Wang[1,2], *Shuangde Li*[1,2]*, *Linfeng Nie*[1], *Yunfa Chen*[1,2]*

1 State Key Laboratory of Mesoscience and Engineering, Institute of Process Engineering, Chinese Academy of Sciences, Beijing 100190, People's Republic of China.

2 University of Chinese Academy of Sciences, No. 19A Yuquan Road, Beijing 100049, People's Republic of China.

*e-mail: sdli@ipe.ac.cn, chenyf@ipe.ac.cn

KEYWORDS: Low-temperature water-gas shift reaction, CO activation, H_2O dissociation, Active site design

View Article Online
DOI: 10.1039/D5TA02030A

ABSTRACT

To solve the energy crisis, water-gas shift reaction (WGSR) has been deeply and systematically studied for effectively providing pure hydrogen and removing hazardous carbon monoxide spontaneously. In typical industrial applications, the WGSR commonly consists of two individual processes: high-temperature shift reaction (320-450˚C) for high reaction rate and low-temperature shift reaction (150-300˚C) for high conversion due to their intrinsic thermodynamic and kinetic properties. Owing to the complexity of traditional catalytic system, researchers have made great efforts to seek low-temperature (< 300˚C) reaction catalysts with better performance and energy efficiency. Recent advancements are mainly based on the correlation of catalyst components and reactivities for low-temperature WGSR. However, this work considers different ideas of catalyst design for enhancing low-temperature WGSR performance based on the combination of two half-reactions: water dissociation and carbon monoxide activation, which occur on different active sites. Therefore, only purposeful active site design for the two half-reactions can constitute an efficient catalyst. This review goals to summarize the advances in the recent decade and provides some possible active site design direction for future investigation.

View Article Online
DOI: 10.1039/D5TA02030A

1 Introduction

Hydrogen (H_2) is widely recognized as a potential clean energy carrier, which could help reduce greenhouse gas emission. Number of hydrogen production process have been developed and studied by scientists, among which water-gas shift reaction (WGSR) is considered as a typically efficient way to produce and purify H_2[1] and it has been applied to many industrial processes, such as natural gas reforming, ammonia synthesize[2] and fuel cell application[3, 4].

The history of WGSR can be traced back to 1780s with their reaction depicted in the following equation: $CO + H_2O \leftrightarrow CO_2 + H_2$ (ΔH_r^θ = -41.1 kJ·mol^{-1}). As an exothermic reaction, it is thermodynamic suitable at low temperature with strict kinetic limit. Therefore, conventional WGSR system contained two adiabatic stages: high-temperature stage with Fe-Cr catalyst for high reaction rate and low-temperature stage with Cu-Zn-Al catalyst ($<$300℃) for forward conversion[5, 6]. The reaction was not applied until 1888 that Mond utilized it for hydrogen production for fuel cell application. In 1914, Bosch and Wild had applied the reaction to industrial hydrogen production[7]. Because of the poisonousness of Cr and the high energy consumption, scientists struggled to optimize the performance of Fe-based catalysts by introducing different kinds of adjuvants until 1980s[8]. But the complexity and energy consumption of the system still encouraged scientists to develop new-style catalytic systems.

View Article Online
DOI: 10.1039/D5TA02030A

Encouraged by the proposal of associative mechanism and redox mechanism in 1920 and 1940[1], scientists realized that the reaction is mainly induced by the interfacial sites between loaded metals and the supports on the heterogeneous catalysts[9]. Increasing kinds of metal oxides are revealed by researchers with decent water dissociation performance and mild reaction condition, such as Al_2O_3[10, 11], $CuFe_2O_4$[12], ZrO_2[13], $CeZrO_4$[14]. Also, the catalytic performance can be assisted by additives such as ZnO[15], Nb_2O_5[16] which adjusting the physical and electronic structure of catalysts. Besides metal oxides, some advanced functional materials were noticed by researchers for their exclusive properties. For example, noble metal based catalysts putting α-MoC as a carrier was emphasized in the last few years for the excellent water dissociation activity[17].

With the development of catalyst design strategies[18], noble metal based catalysts aroused much attention in this field[19, 20]. With moderate adsorption capacity for CO, metals like Au, Pt, Ru, Pd, Ag are frequently selected as active components for WGSR[21, 22]. Furthermore, in 2011, Zhang et al. firstly realized a single atom catalyst (SAC) that consists of single Pt atoms uniformly dispersed on a FeO_x support[23]. With decent catalytic activity and new reaction mechanisms, SACs were further explored for better synthesis methods and catalytic properties and regarded as promising catalysts for WGSR[24]. However, in some occasions, nanoparticles show significant catalytic activity, whereas single atoms act as spectators[25]. It is necessary to differentiate the function of nanoparticles and single atoms in different catalyst system for CO activation.

74 Table 1 Summary of the review perspective and proposed catalyst and active site design approach of some published reviews and this work

Title	Published Year	Review Perspective	Proposed Catalyst and Active Site Design Approach	Ref.
For more and purer hydrogen-the progress and challenges in water gas shift reaction	2023	Catalyst type and catalyst structure	Low and high temperature shift reaction catalysts Sulfur-tolerant and wide temperature shift reaction catalysts Nano catalysts and Single-atom catalysts design Surface structure design	1
The water gas shift reaction: Catalysts and reaction mechanism	2021	Catalyst component	Fe-based catalysts Cu-based catalysts Ni-based catalysts Co-Mo-based catalysts Noble-metal-based catalysts	8
Noble-metal based single-atom catalysts for the water-gas shift reaction	2021	Catalyst component and active species (noble-metal-based catalysts)	Single-atom catalysts with reducible oxide, irreducible oxide, carbides and nitrides supports Active metal species (positive state and metallic state)	21
Platinum based catalysts in the water gas shift reaction: Recent advances	2020	Catalyst component and mechanism study (platinum-based catalysts)	The influence of supports The influence of loading method and loading amount The influence of promoter addition Kinetic and mechanism study of Pt-based catalysts	22

The review of Cr-free Fe-based catalysts for high-temperature water-gas shift reactions	2013	Catalyst component (Fe-Cr-based catalysts)	Iron oxide-Chromium oxide catalysts Chromium free catalysts	7
Water gas shift catalysis	2009	Catalyst component	Iron oxide-Chromium oxide and Chromium free catalysts for high temperature shift reaction Cu-Zn-Al and promoted Cu catalysts for low temperature shift reaction Sulfur-tolerant catalysts Noble-metal-based catalysts Monolith-coated catalysts for fuel cell	
The water-gas shift reaction	2006	Catalyst component and kinetic study	Iron-based shift catalysts Copper-based shift catalysts Cobalt molybdenum-based shift catalysts	6
Reasonable active site design for promoting water dissociation and carbon monoxide activation in low temperature water-gas shift reaction	**/**	**Mechanism summary and active-site-design strategy for the two half-reactions of WGSR**	**Mechanism study of WGSR** **Active site design strategies for H_2O dissociation** **Active site design strategies for CO activation**	**This work**

View Article Online
DOI: 10.1039/D5TA02030A

Up to now, most WGSR reviews mainly focus on the correlation between different catalyst structure and performance, like noble metal catalysts, transitional metals-based composite and so on. For example, Zhou et al. discussed different sorts of supported metal nanoparticle catalysts for WGSR[1] and Chen et al. detailly summarized noble-metal-based single-atom catalysts for WGSR[21]; Pal et al. provided a systematical review for transitional-metal-based catalysts[26]. Lee et al. focused on the impacts of reaction conditions and catalysts on WGSR involving different feed gases[27]. Some other reviews with their review perspectives and proposed catalyst and active site design approaches have been summarized in Table 1. These reviews demonstrated comprehensive understanding of different catalytic systems and summarized the promising catalysts in terms of material composition. However, to our best knowledge, few reviews conduct their discussion based on the understanding of active site design, which triggered us to summarize the first-class catalyst designs and attempt to find some possible correlation between active site structure and promising catalytic performance. More importantly, based on the proposal of surface catalytic theory[28] and the specificity of the WGSR, this review considered it as the combination of two principal half-reactions: water dissociation and CO activation, and emphasized that most excellent catalyst design strategies focused on at least one of the half-reactions, whose significancy was hardly acknowledged by the previous reviews as shown in the last row of Table 1. Additionally, on knowing that the deactivation of catalysts is still an inevitable phenomenon in actual

View Article Online
DOI: 10.1039/D5TA02030A

situation, some typical active site design strategies aimed at the inhibition of deactivation, which is worth discussing with their specific examples in this review.

2 Mechanisms

The studies on the mechanism of WGSR have been conducted for a few decades because it is complex and still remain controversial. The most recognized mechanisms can be roughly divided into two categories, which mainly involves different routines of water dissociation and carbon monoxide activation: redox mechanism and associative mechanism.

The redox mechanism was first proposed by Temkin in 1949[29]. The shift reaction goes through a redox cycle as shown in the schematic in Figure 1 (a) and Eq. 1-5, where * represents the active site. To be specific, the H_2O will be directly adsorbed and activated on the active sites to be thoroughly dissociated into H_2 and O* (light blue balls: H atoms; dark blue balls: O atoms dashed circle: oxygen vacancy; grey rectangle: support) and consume much energy. Simultaneously, the CO will be activated and react with the lattice oxygen to generate CO_2, leaving an oxygen vacancy which will be supplied by the O* from H_2O (black balls: C atoms; light yellow balls: low valance state noble metals; dark yellow balls: high valance state noble metals; yellow ellipse: noble metal sites). The reduction process is entirely independent from CO oxidation, and need enough activation energy to be thoroughly dissociated. Therefore, this mechanism is more favored by high-temperature shift reaction and active sites with better reduction capacity.

View Article Online
DOI: 10.1039/D5TA02030A

$H_2O + * \rightarrow H_2O^* \rightarrow H^* + {}^*OH \rightarrow 2H^* + O^*$ Eq. 1

$O^* + O_V \rightarrow O_L$ Eq. 2

$2H^* \rightarrow H_2$ Eq. 3

$CO + * \rightarrow CO^*$ Eq. 4

$CO^* + O_L \rightarrow CO_2 + O_V$ Eq. 5

With the research trend for lower reaction temperature, the associative mechanism based on Langmuir-Hinshelwood model gradually came into scientists' eyesight. As shown in the schematic in figure 1 (b), different from the redox mechanism, the water dissociation will only be partially dissociated into H* and *OH, and the *OH will further react with CO* to generate important free radical intermediates such as carboxyl (*COOH) and formyl (HCOO*), thus the reduction and oxidation processes are not independent but associative. The intermediates will decompose into CO_2 and an extra H*, which can combine with the former H* to produce H_2. This mechanism described by Eq. 6-9 revealed that the *OH could directly react with activated CO and form important intermediates which could be further reform into CO_2 and H_2, rather than indispensable exhaustive dissociation into O* and H* with higher activation energy, resulting in lower reaction temperature.

$H_2O + * \rightarrow H_2O^* \rightarrow H^* + {}^*OH$ Eq. 6

$CO + * \rightarrow CO^*$ Eq. 7

$CO^* + {}^*OH \rightarrow {}^*COOH \rightarrow CO_2 + H^*$ Eq. 8.1 (Carboxyl-Intermediate Pathway)

$CO^* + {}^*OH \rightarrow HCOO^* \rightarrow CO_2 + H^*$ Eq. 8.2 (Formyl-Intermediate Pathway)

View Article Online
DOI: 10.1039/D5TA02030A

138 $2H^* \rightarrow H_2$ Eq. 9

139 Both mechanisms above could be credible under different conditions with different
140 rate determining steps (RDS). For example, WGSR on classic high-temperature
141 catalysts like Fe_3O_4 composite tend to follow the redox mechanism. Huang et al.
142 conducted meticulous density functional theory calculation using Fe_3O_4 (111) surface
143 with the $Fe_{oct2\text{-}tet1}$ terminal and proved that redox mechanism was the primary reaction
144 routine with the RDS of CO_2 desorption because of the distinguishing water adsorption
145 ability of Fe_{oct2} sites[30]. Nevertheless, noble metal catalysts with abundant well-designed
146 interfacial active sites allowed easy combination of CO* and *OH, leading to the
147 associative mechanism. Vecchietti et al. studied Pt/CeO_2 catalyst and diffused
148 reflectance infrared Fourier transform spectroscopy (DRIFTS) results demonstrated the
149 existence of HCOO* and COO* species, which are typical intermediates of associative
150 mechanism. They also mentioned that on the contrast of the previous research, the
151 activation of water molecules in the WGSR mechanism is not the RDS in this system[31].
152 These previous works emphasized the complexity of the reaction mechanisms with
153 various catalytic systems and reminded the future researchers that reasonable designing
154 of the interfacial site that initiated associative mechanism might be a common solution
155 for the first-class catalysts. Considering that the water dissociation and CO activation
156 are both inevitable for WGSR, these two vital processes could be thinking pivots for
157 the future active site design strategies, which would be further discussed in the
158 following section of the review.

View Article Online
DOI: 10.1039/D5TA02030A

3 Active sites design

3.1 Water Dissociation

Water dissociation is the key process of H_2 production and active intermediate generation in WGSR. Metal oxides have been widely studied in laboratory and industrial process for water dissociation. As a kind of common defect site on the surface of oxide catalysts, oxygen vacancies are regarded as the reaction sites and it has been investigated for a long time because of its high activity and stability[32]. Mostly, the activity of oxygen vacancies can be influenced by two factors: concentration and species. Also, some metal sites can undertake the task of water dissociation by purposive catalyst design. Therefore, it is worthwhile summarizing the ideas for active sites design, which can be demonstrated in Figure 2.

3.1.1 Oxygen Vacancy

3.1.1.1 Concentration of Oxygen Vacancy

For the reducible metal oxide supports, such as CuO[33], Fe_2O_3[34], TiO_2[35], CeO_2[36] and so on, the concentration of oxygen vacancy can be easily controlled by synthesizing and pretreatment methods such as element doping. Jeong et al. prepared a series of Cu-CeO_2-ZrO_2 materials with different Ce/Zr ratio. They found that by the shrinkage of lattice, Cu-$Ce_{0.8}Zr_{0.2}O_2$ contained a larger amount of oxygen vacancies and exhibited a very stable WGSR activity at about 300°C, which is correlated with the enhancement of oxygen mobility. This work also mentioned that compared with tetragonal phase of Cu-$Ce_{0.8}Zr_{0.2}O_2$, cubic phase shows higher WGSR activity because it helps to achieve

View Article Online
DOI: 10.1039/D5TA02030A

higher concentration of oxygen vacancy[14]. Homogeneously, the design of La doped CeO_2[37, 38] and Ga doped Pt/CeO_2[31] achieved high concentration of oxygen vacancy and thereby promoted catalytic activity for WGSR. Therefore, element doping is regarded as a valid performance-promoting pathway[39]. And similarly, the synthesis condition of catalysts can also change the O_V concentration, which needs to be further discussed.

In summary, there are direct evidences showing that materials with more oxygen vacancies tend to be more active in water dissociation process, because oxygen vacancies serve as the main active site of water dissociation and can stabilize the *OH, which enhance the WGSR activity.

3.1.1.2 Species of Oxygen Vacancy

Apart from gaining higher concentration of oxygen vacancy, recent advanced works mainly focus on the species of oxygen vacancy. Zhou* et al. successfully formed an asymmetric environment of oxygen vacancies also by element doping[32]. For example, the group doped Bi in CeO_2 and modified the surrounding of the oxygen vacancy by forming a distorted tetrahedral geometry of $Bi\text{-}O_v\text{-}Ce_3$. In comparison with traditional symmetric clusters like $Ce_2\text{-}O_v\text{-}Ce_2$, the asymmetric oxygen vacancy makes both the adsorption and desorption much easier (Figure 3 (a))[40]. It is predictable that such asymmetric oxygen vacancy can be applied to some structure-sensitive reaction like the activation of H_2O in WGSR.

Researchers obtained a Zn-Ti mixed oxide support from a Zn-Ti layered double hydroxides precursor. Because of the strong metal-support interaction, after loading Au

View Article Online
DOI: 10.1039/D5TA02030A

nanoparticles, the electrons will transfer from the TiO_{2-x} overlayer to Au atoms to form the asymmetric oxygen vacancy site $Au^{\delta-}$-O_v-Ti^{3+} shown in Figure 3 (b), and deep analyzation of X-ray absorption near edge structure (XANES) results shown in Figure 3 (d) provided convincing evidence of the asymmetric oxygen vacancies. During the WGSR, both $Au^{\delta-}$ and O_v species of the site directly participate in the H_2O dissociation process. Moreover, characterization results substantiated that the active oxygen vacancy also accelerated the CO chemisorption and H_2O dissociation[41]. The group also reported a TiO_{2-x}-modified Ni catalyst with tunable Ni-TiO_{2-x} interaction and the reaction process over $Ni^{\delta-}$-O_v-Ti^{3+} site was discussed. By the in situ time-resolved DRIFTS results, a new redox mechanism was revealed and can be illustrated by two main steps: (1) the cleavage of O-H bond in H_2O molecule at the asymmetric oxygen vacancy site to generate H_2 and transform $Ni^{\delta-}$-O_v-Ti^{3+} into $Ni^{\delta+}$-O-Ti^{4+}; (2) reaction between CO and $Ni^{\delta+}$-O-Ti^{4+} to form CO_2 and $Ni^{\delta-}$-O_v-Ti^{3+}. These works focus on the establishment of asymmetric active oxygen vacancy and provide a new possible solution for construction of high-efficiency heterogeneous catalytic systems[42, 43]. Many other works have successfully synthesized composites with asymmetric oxygen vacancies which also exhibited LT-WGSR performance[44].

Additionally, based on the design of asymmetric oxygen vacancy, Chen et al. synthesized a bilayer Cu covered on CeO_2 (structure illustrated by Figure 3 (c)). The bottom layer of Cu can donate an electron to Ce^{4+} and coordinate with an O_v to form a Cu^{+}-O_v-Ce^{3+} site, and the top layer of Cu can bond with the underlying Cu^{+} to modify

View Article Online
DOI: 10.1039/D5TA02030A

the site to Cu^0-Cu^+-O_v-Ce^{3+}. Such interfacial active sites can optimize the plane-integrated bonding charge shown in Figure 3 (e) around Cu^+ and O_v sites, thereby enhance the CO adsorption and H_2O dissociation capacity[45].

Although the oxygen vacancy concentration is an important factor for the catalytic performance, the optimization of it is capped by the stability requirement of catalysts. Designing better oxygen vacancy species like the asymmetric oxygen vacancy is more crucial for more efficient catalytic system and can fundamentally reveal the H_2O dissociation mechanism.

3.1.2 Metal site

Except for oxygen vacancies, metal sites can also play as the core sites for water dissociation. For traditional metal oxide catalysts, the loaded metal can be the water adsorption sites, and the dissociation capacity can be enhanced by the establishment of the interfaces between laded metals and supports. Lucas et al. designed a Ni/Al_2O_3 composite and deeply tracked the oxygenate species (O* and *OH) from water dissociation process at interface sites in contrast to the bare Ni surface. They found that the surface species are only available at the interfacial sites. The results reminded us that the combination of metal and support can be properly adjusted to obtain better water dissociation activity, and the WGSR is a typical interface-sensitive reaction[11].

Plentiful studies center on MoC for production of high-purity H_2 was carried out and achieved intriguing advances[46, 47]. Different from other oxides like SiO_2 or TiO_2 which cannot dissociate H_2O or can easily dissociate H_2O into H^+ and OH^- respectively, the

View Article Online
DOI: 10.1039/D5TA02030A

mass spectrum results have shown that after being adsorbed on α-MoC, the H_2O can be instantly dissociated into H* and *OH at almost room temperature, which are both important intermediates for WGSR[48]. Researchers composed a review to summarize the efforts they made on the development of M/MoC. The review mentioned that the wonderful catalytic performance of MoC originated from the incorporation of carbon atoms at the interstitial sites, which endows MoC with higher density of states near the Fermi level and proper electronic interaction between carbon atoms and metals. Such electronic interaction can optimize the adsorption energy of H_2O to a moderate level where the H_2O molecular can be solidly adsorbed on the surface and simultaneously dissociated by the energy released from adsorption[49]. Furthermore, Zhang et al. designed Pt_1-Pt_n/α-MoC (morphology and structure shown in Figure 4 (a)) based on Pt_1/α-MoC with promising activity but disappointing stability and obtained better CO conversion than Cu-Zn-Al model catalyst and other MoC-based catalysts given in Figure 4 (b). The extra Pt clusters can change the interfacial structure by covering the redundant exposed surface of Pt_1/α-MoC, in order to preventing the oxidation of α-MoC by excess *OH, because the *OH far from the interface of Pt and α-MoC cannot react with the activated CO. Also, the transient kinetic analysis (TKA) results of Pt_1-Pt_n/α-MoC revealed that except for H_2O dissociation, the CO can also be dissociated at low temperature to generate an extra carbon atom which can react with activated H_2O to produce additional 35% of H_2 in the total H_2 production. The reaction routines can be summarized by Figure 4 (c). By isotope labelling method, this work found some

View Article Online
DOI: 10.1039/D5TA02030A

different reaction routines based on the dissociation of CO, which means that the combination of noble metal and α-MoC can not only make full use of the water dissociation capacity of MoC, but also enhance the CO activation process, resulting in more active oxygen species supplement from CO dissociation[50]. The fantastic performance of α-MoC based catalysts provided possibility for future research to investigate the electronic structure optimization of metal sites, in order to improve intrinsic H_2O dissociation ability, but there might be still many challenges to surpass the current performance of the α-MoC based catalysts.

MoC has been proved as an outstanding H_2O dissociation material, and other carbides like TiC[51, 52] and Co_2C[53] are also under investigation. Additionally, metal-organic frameworks (MOFs) have been predicted as promising supports with controllable porous structure and changeable open metal sites (OMSs) [54]. However, limited MOFs have been applied in LT-WGSR because of their instability in vapor atmosphere. Recently, Rivero-Crespo et al. synthesized a robust and highly crystalline MOF which can stabilize Pt^+ single atom sites by a water cluster. The work reported a double water attack mechanism for the MOF to give CO_2, in which both of the oxygen atom in CO_2 are coming from H_2O. However, the synthesis of the MOF is complex and time-consuming, which needs further development[55].

The optimization of metal sites mainly focuses on adjusting the electronic structure by adjusting the surrounding environment. No matter loaded metal sites or support metal sites, it is vital to reveal the volcano-type relationship between metal sites and

View Article Online
DOI: 10.1039/D5TA02030A

surrounding atoms, which can really provide valid active site design reference for future research.

3.2 Carbon Monoxide Activation

Meanwhile, carbon Monoxide activation is essential for CO elimination in WGSR. Sometimes oxygen vacancy can serve as CO adsorption site at the interfacial zone between loaded metal and supports, but in most LT-WGSR process, d-block elements, such as noble metals, can perform as the effective CO activation sites by cooperate with the supports[56, 57]. Opinions on how to optimize the activation sites for better performance remains unclear and contradictory. In this section, optimizing the geometric structure and electronic structure are considered as two feasible choices for the enhancement of d-block element performance (shown in Figure 5), which will be discussed below.

3.2.1 Geometric Structure

The geometric structure can directly affect the catalytic performance by changing the interaction between catalysts and substrates. For instance, metal loaded on supports can be controllably synthesized with varies of sizes, such as nanoparticles, clusters and single atoms[58]. And based on the size effect, different sizes exhibited different catalytic performance and stability. Also, exposed facet of the catalysts is a key factor to the catalytic performance[59]. It is essential to summarize the merits and drawbacks of different geometric structures, in order to provide clear strategies for reference.

View Article Online
DOI: 10.1039/D5TA02030A

Generally, it is well-known that as the maximization of interfacial site, single atom catalysts should be divinely high-efficiency for WGSR. However, works have been delivered to identify the active sites of CO activation and prove that nanoparticles performed better than single atom by time-dependent infrared spectrum. The result proved that only CO adsorbed on Pt nanoparticles could be activated and participate in the reaction (demonstrated in Figure 6 (a)) [25]. Therefore, with decent catalytic performance and stability, they are widely investigated for LT-WGSR since 1996[19, 34]. Andreas et al. designed TiO_2-supported Pt catalysts and used density functional theory (DFT) calculations and microkinetic modeling to clarify the activity of the three-phase boundary. Their results suggested the dominant catalytic process on $Pt_8/TiO_2(110)$ should be redox pathway and the better activity of three-phase boundary can be correlated to reduced CO adsorption energy on Pt sites and increased number of oxygen vacancies[59]. Moreover, Zhao et al. synthesized a Pt-TiO_2 composite with ultra-small Pt nanoparticles encapsulated in sub-50 nm hollow TiO_2 nanospheres. With the decrease of Pt particle size, the catalyst shows a much higher turnover frequency (TOF) value, which can be attributed to the size-dependent variation in the electronic structure of Pt species and the sintering prevention effect from TiO_2 encapsulation. This work provided a valid synthesis strategy for loading Pt on the internal surface of TiO_2 nanospheres and revealed a creative catalyst designing thought that the deactivation of Pt could be avoided by controllable support encapsulation[60]. CeO_2 is a typical reducible support and is frequently selected as the support of noble metals such as Au[61]. Fu et al.

View Article Online
DOI: 10.1039/D5TA02030A

compared the activity of Au nanoparticles and clusters on CeO_2 and found that the abundant interfacial sites between Au clusters and CeO_2 induced superior catalytic performance than Au nanoparticles during WGSR[62]. In short, the size of loaded metals could directly determine the number of active sites.

Zhang et al. synthesized Pt clusters and single atoms by changing the loaded facets shown in Figure 6 (b). They deeply investigated the CO adsorption on Pt by IR spectrum given in Figure 6 (c) and proved that the binding energy between CO and Pt nanoparticles is weaker than CO and Pt single atoms by the blue shift of PtO_4^{2+} peak compared with $Pt^{\delta+}$ and Pt^0 peaks, which means that single atom catalysts (SACs) could be well designed to show promising research value[63]. Therefore, for WGSR, single atom sites with appropriate geometry design can still effectively activate CO for further reaction with other intermediates such as *OH. Lin et al. synthesized Ir_1/FeO_x SAC for WSGR whose performance is one order of magnitude higher than its cluster and nanoparticle counterparts[64]. Furthermore, Liang et al. studied the redox mechanism of Ir_1/FeO_x for WGSR by detailly calculation and experiments and proved that the CO will be adsorbed and activated on the Ir single atom with a dual active site of Fe^{3+}-O···Ir^{2+}-O_v[65]. And Guan et al. from the same group also fabricated Rh_1/TiO_2 SAC and obtained an overall CO conversion of ~95%, which indicated that there are multiple choices of noble metal for LT-WGSR[66]. Some kinds of SACs have also broken the traditional cognition that noble metal sites are the actual CO activation sites. Sun et al. designed a Ir_1/α-MoC catalyst for LT-WGSR. Different from other works, they revealed that the

View Article Online
DOI: 10.1039/D5TA02030A

great performance does not originate from the direct participation of Ir single atoms in the CO activation. The Ir single atoms served as a promoter which assisted Mo sites to activate CO. With kinetic measurements and theoretical calculation, they proved that the addition of Ir single atoms effectively changed the electronic property of Mo sites, resulting in a obviously reduction of the activation energy (E_a)[67]. These works provided abundant possibilities for the utilization of SACs in the future research with rational catalyst design to avert excessively adsorption.

As for the influence of exposed facets, Zhang et al. synthesized uniform cubic, dodecahedral and octahedral Cu nanocrystal by partial reduction of Cu_2O nanocrystal. They found that cubic Cu nanocrystal exposed (100) facets was more active than dodecahedral Cu nanocrystal exposed (110) facets for H_2O dissociation and CO activation, and octahedral Cu nanocrystal exposed (111) facets was inactive. By theoretical calculation results of surface structures and H_2O adsorption energy change, it is confirmed that the formate species adsorbed on Cu (111) need to overcome a large barrier to decompose, leading to the accumulation of formate and finally covering the active sites. Therefore, the Cu (111) facets are initially active, but will be self-poisoning during the reaction[68]. On the basis, the research group deeply studied ZnO/Cu and revealed that the catalysts would undergo an in situ restructuring process during WGSR to form the Cu-hydroxylated ZnO ensemble[69]. These results suggested that controlling the exposed facet of crystalized catalysts like traditional Cu-based catalysts might also be a considerable strategy for performance optimization.

View Article Online
DOI: 10.1039/D5TA02030A

As is shown above, a reasonable geometric structure is important for better catalytic performance. The size and morphology effect need to be detailly investigated and discussed based on the experience and future works, aiming to summarize some universal catalyst design rules.

3.2.2 Electronic Structure

3.2.2.1 Strong metal-support interaction (SMSI)

The Strong Metal-Support Interaction (SMSI) was first found by S.J.Tauster and S.C.Fung in 1978[70]. The interaction broadly exists in numerous kinds of supported catalysts and markedly adjusts their electronic structure, such as the electron states of loaded metals. For example, as we mentioned in water dissociation section, SMSI can optimize the electron distribution of metal sites. Similarly, Abdel-Mageed et al. employed operando X-ray absorption spectrum (XAS) and FT-IR to identify the active Au species in highly active Au/CeO_2 catalyst. By synthesizing Au species with different electronic states ($Au^{\delta-}$, Au^0, $Au^{\delta+}$) on purpose, they presented an idea that the nanometer-sized Au^0 particles are the dominant active species rather than the cationic Au species (Au^{3+})[71]. Apart from that, the coordination number of active sites is related to the strength of SMSI. Jin et al. loaded Au atomic layers and isolated atoms on MoC to synthesize different Au/MoC catalysts. With XAS analysis and catalytic performance test, they revealed a volcano-style pattern between the specific activity for LT-WGSR and the coordination number of Au-Au. These results offered a reference for the geometric and electronic structure design in the future[72]. The SMSI designed in these

View Article Online
DOI: 10.1039/D5TA02030A

works noticed us that for better CO activation performance, the interaction should be moderate. Excessively weak SMSI cannot form qualified active sites and the CO molecules are uneasy to react with oxygenate species if the SMSI is too strong.

In order to obtain an appropriate SMSI between loaded metals and supports, scientists offer varieties of methods. For example, Yang et al. demonstrated the origin of SMSI by using Pt/CeO_2 as a model catalyst and WGSR as a model reaction. On $CeO_2(110)$, Pt clusters embed into CeO_2 lattice within 3-4 atomic layers. Such embedding structure optimizes the SMSI between Pt clusters and CeO_2 for more productive Pt sites[73]. Similarly, the Pt/TiO_2 with overlayer structure can also optimize the SMSI[74]. The results remind us that SMSI could be optimized by adjusting the geometric structure of materials.

Another important factor of SMSI is the component and concentration of active sites. Cu/Fe_3O_4 is a simple and non-toxic material. The formation of $CuFe_2O_4$ spinel structure can enhance the thermostability and change the electronic state of Cu and Fe by Jahn-Teller effect[75]. Lin et al. prepared a Cu/Fe_3O_4 catalyst by co-precipitation method to gain larger amount of $CuFe_2O_4$, better which were responsible for CO activation[33]. Han et al. further optimized the composition of Cu/Fe_3O_4 and found the $Cu_{0.3}Fe_{0.7}O_x$ exhibited the highest CO conversion. The group reported that excessive loaded Cu will sinter and insufficient loaded Cu will suffer from lack of active sites and poisoning[12]. For future investigation, it is necessary to figure out the most applicable component for a promising material.

View Article Online
DOI: 10.1039/D5TA02030A

3.2.2.2 Synergistic effect

Besides normal nanoparticle-based materials, bimetallic sites and alloys arouses much more attention because the synergistic effect between two different metals is intriguing and contains profound scientific principles[76, 77]. Recent research trend of bimetallic catalysts for WGSR focus on the bimetal size adjustment and composition optimization to reduce the cost and enhance the performance[78-80]. As typical active components, Cu and Ni can be loaded on Fe_2O_3 simultaneously. The H_2-TPR results indicated that the SMSI between the dopants (Cu or Ni) and Fe_2O_3, which was beneficial to LT-WGSR[81]. Zhang et al. anchored well-dispersed Pt single atoms on Co_3O_4 nanorods, forming a Pt_1Co_n/Co_3O_4 composite shown by structure schematic in Figure 7 (b), and found that the singly dispersed Pt_1Co_n nanoclusters were the active sites of WGSR in the temperature range of 150-200˚C. After increasing the temperature to about 300˚C, the Co_3O_4 demonstrated by Figure 7 (a) will be reduced to CoO_{1-x} and Pt will sinter, resulting in the formation of $Pt_mCo_{m'}/CoO_{1-x}$ demonstrated by Figure 7 (c) with more abundant surface oxygen vacancies. Both H_2O dissociation and CO activation process take advantage of the $Pt_mCo_{m'}$ active sites and achieve a lower activation energy, which suggested a effective method to tune the reactivity through reconstructing the oxide catalyst in the gas phase[82]. Xia et al. prepared Au and AuM (M=Ni, Cu, Pt) alloy nanoparticles supported on layered double hydroxides (LDHs) and found Au_2Cu_1 exhibited the highest TOF value with modulation to the redox process at the interface of AuM/LDHs interfaces[83]. These works of bimetallic catalysts

View Article Online
DOI: 10.1039/D5TA02030A

431 construction with optimized structure show great potential for LT-WGSR, but the type
432 and structure of metals need to be carefully designed for reacting in concert.

433 As a kind of electronic adjuvants, alkali elements are often doped in some supported
434 catalysts to optimize the electronic structures of metal sites. Therefore, many noticeable
435 works have been reported and provided plentiful solutions. Au loaded on zeolites and
436 mesoporous MCM-41 were found to be stabilized by the addition Na^+ and K^+. The
437 single site species of Au-$O(OH)_x$-(Na or K) are active for the LT-WGSR below 200˚C,
438 and the $AuO_{6-7}(OH)_2Na_9$ clusters exhibited the best catalytic performance and
439 stabilization with the applicable CO adsorption energy because the addition of alkali
440 ions performed as an electron acceptor and shared part of the electrons transferring to
441 Au atoms to form a moderate Bader charge on Au[84]. Coincidentally, Pt-Na/SiO_2 has
442 also been synthesized and showed better activity than Pt/SiO_2 below 300˚C[25]. Kaftan et
443 al. applied DRIFTS coupled with online quadrupole mass spectrometry (QMS) to
444 observe the formation of surface species and demonstrate the enhancement of KOH
445 coated Pt/Al_2O_3. They assured that formates are the primary intermediate on uncoated
446 Pt/Al_2O_3, while a film of hydroxides and carbonates is observed on the KOH-coated
447 sample. It is interesting that the change of electronic structure by alkali species can
448 affect the dominant routine of WGSR. Additionally, the strong red shift of CO
449 adsorption peak in DRIFTS suggested that K-coadsorption can weaken the C-O bond
450 and strengthen the Pt-C bond, leading to hinderance for CO desorption and facilitation
451 for the reaction of CO with *OH[85]. Ang et al. suppressed the formation of methane by

View Article Online
DOI: 10.1039/D5TA02030A

covering a layer of Na/NaO_x on Ni loaded CeO_2. The Na^+ could replace the Ce^{4+} in the lattice and generate abundant lattice defects thus increasing the oxygen mobility, which will make the redundant CO adsorbed on Ni rapidly degraded and prevent the catalyst from being poisoning[86]. These works revealed that the alkali metal doping can change the electron distribution of catalysts, in order to enhance the performance of active sites and change the reaction routine.

Generally, the electronic structure of active sites can be adjusted by bimetallic site design and alkali doping based on the synergistic effect between the metals. For different sites with different performances, they need concrete analyses of their specific situations to ensure that which elements can help to achieve the best optimization results.

4 Summary and Prospect

Being regarded as a promising reaction fulfilling two expectations of converting CO and generating H_2 simultaneously, WGSR is a promising reaction but faces the problem that the temperature cannot overcome the thermodynamic and kinetic limits synchronously, thus bunches of catalytic systems have been developed for high-efficiency WGSR. In this review, we considered WGSR as a combination of two half-reactions: H_2O dissociation and CO oxidation, which are the optimization targets of active sites design. The combination of active site design for the two side reactions makes high-efficient WGSR for CO removal and H_2 production possible. In the past one-decade, numerous research has achieved important advances in the following prospects. For water dissociation, the concentration and structure of oxygen vacancies

View Article Online
DOI: 10.1039/D5TA02030A

can be designed for better catalytic performance and reasonable metal sites design can help them efficiently participate in the process. For carbon monoxide activation currently happening on d-block element sites, selectively synthesizing suitable size and exploring providential electronic structure of the sites are both considered as valid ideas for designing first-class catalysts. Some catalysts stood out with promising activity and industrial application potential, such as noble metal loaded on CeO_2, α-MoC. But the comparing with the relatively mature applied catalysts like Cu/Zn/Al system, the harsh synthesis process and costly ingredients hindered their industrial application prospects and research on the resistance of catalyst deterioration need to be further conduct in the future. The future active site design strategies should take the industrial costs and production scenarios into consideration and target at economical, stable and efficient catalytic system.

Taken together, although WGSR has been investigated for a long period of time, there is still room for improvement of the catalytic systems, which triggered extensive interest from the scientific community. With the proposing of more novel theories and the development of large language model, the catalysts for WGSR also need to stay up-to-date and the designing methods could be assisted by AI prediction. We hope that the development of active sites design for WGSR can make it a really efficient pathway for H_2 generation and CO oxidation in the future.

View Article Online
DOI: 10.1039/D5TA02030A

492 **FIGURES**

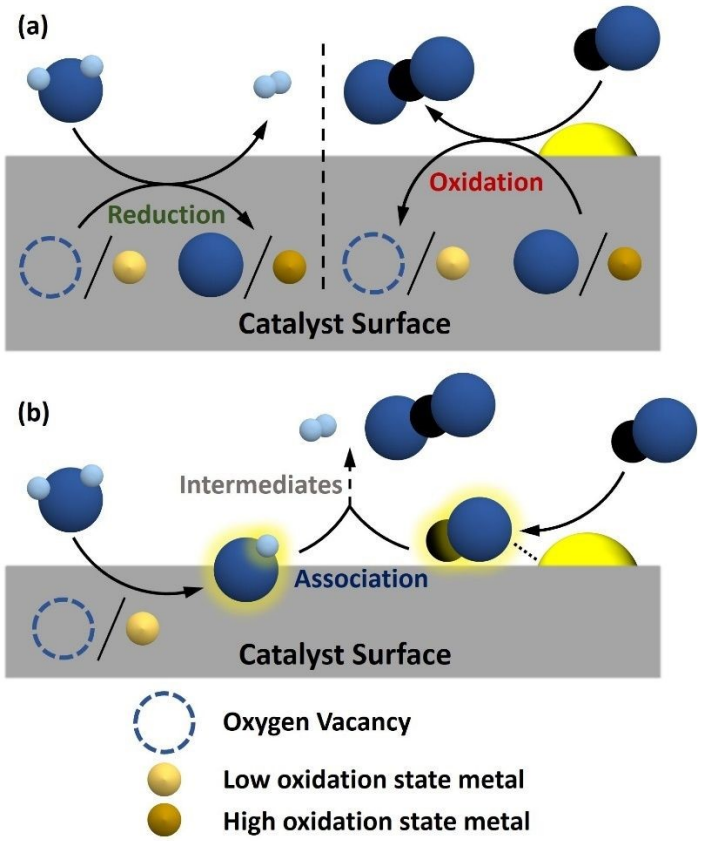

493 **Figure 1** (a) Process schematic of redox mechanism. (b) Process schematic of

494 associative mechanism.

495

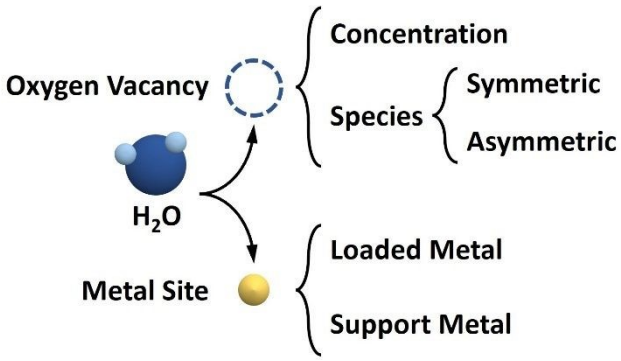

496 **Figure 2** Summarization of active site design for H_2O dissociation.

497

498

View Article Online
DOI: 10.1039/D5TA02030A

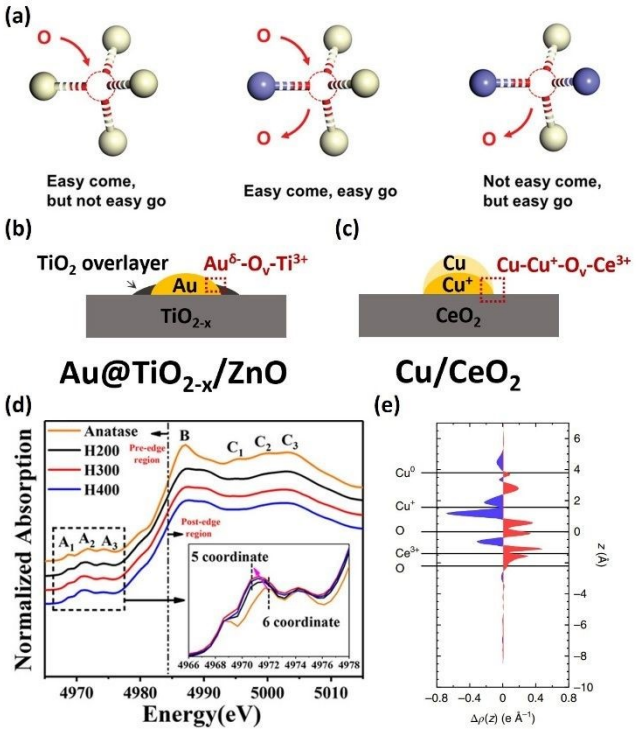

500 **Figure 3** (a) Schematic diagram of relationship between the microstructure of oxygen
501 vacancy and its redox property. (b) A diagram of the active site structure on Au@TiO_{2-}
502 $_x$/ZnO. (c) A diagram of the active site structure on Cu/CeO_2. (d) Normalized XANES
503 spectra of Au@TiO_{2-x}/ZnO with different synthesizing condition, which provided a
504 direct evidence for the existence of asymmetric oxygen vacancy site ($Au^{\delta-}$-O_v-Ti^{3+}). (e)
505 Plane-integrated bonding charge $\Delta\rho(z)$ as a function of position across the Cu-Ce
506 interface. The red and blue areas represent charge accumulation and depletion,
507 respectively.

510

511

View Article Online
DOI: 10.1039/D5TA02030A

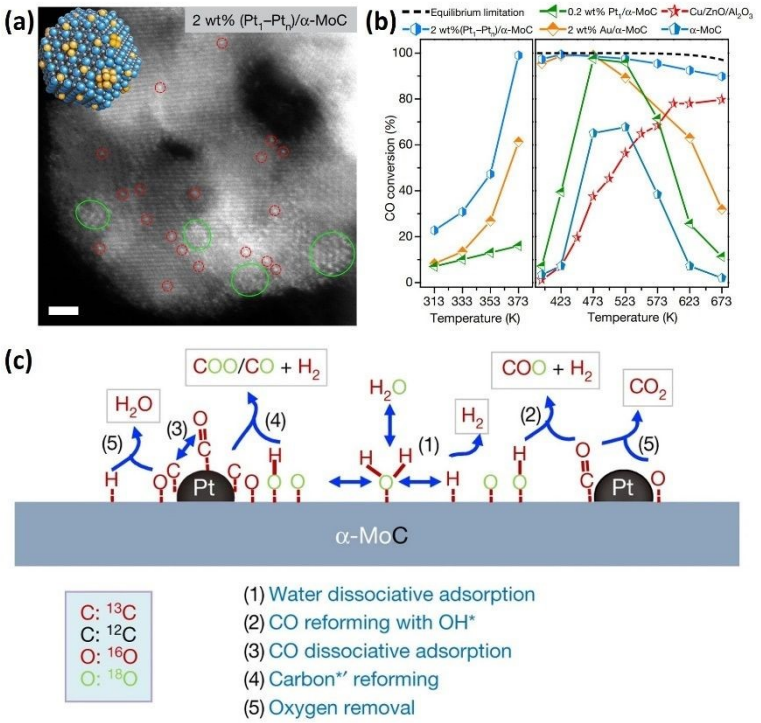

513 **Figure 4** (a) TEM image and a diagram of the distribution of Pt single atoms and clusters
514 on (Pt_1-Pt_n)α-MoC. (b) CO conversion over different catalysts at various temperatures.
515 (c) Schematic of the reaction routes for the WGS reaction over Pt/α-MoC: (1) water
516 dissociation; (2) the conventional WGS reaction routes (redox or associative
517 intermediate mechanism); and (3)–(5) the unconventional WGS reaction routes. The
518 asterisk represents the active site.

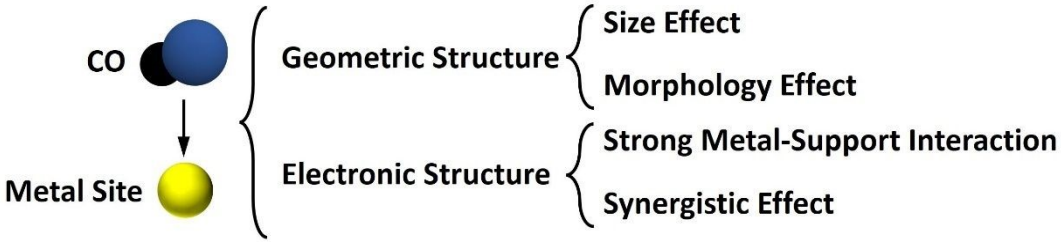

520 **Figure 5** Summarization of active site design for CO activation.

521

View Article Online
DOI: 10.1039/D5TA02030A

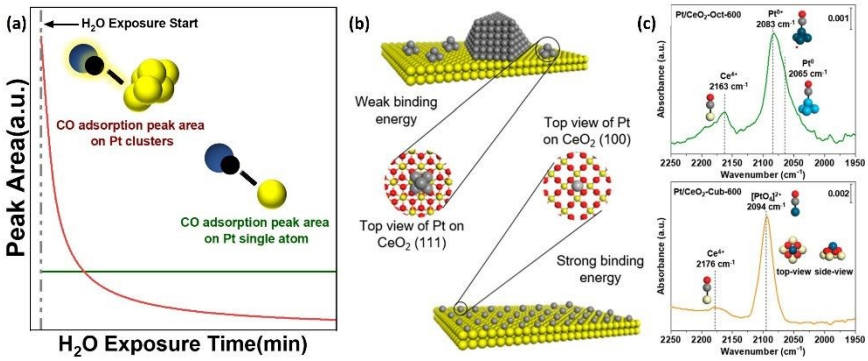

Figure 6 (a) Time-dependent IR spectra of CO adsorbed on 1 wt.% Pt/SiO_2 upon H_2O exposure. The peaks in green zone corresponds to CO adsorbed on Pt single atoms and the peaks in blue zone corresponds to CO adsorbed on Pt nanoparticles. The diagrams on the right side shows the CO activation status on different sites. (b) A diagram of Pt cluster and single atom on different CeO_2 facets. (c) In situ CO-DRIFTS of Pt/CeO_2 samples, showing the bonding energy differences between CO and Pt with different sizes.

View Article Online
DOI: 10.1039/D5TA02030A

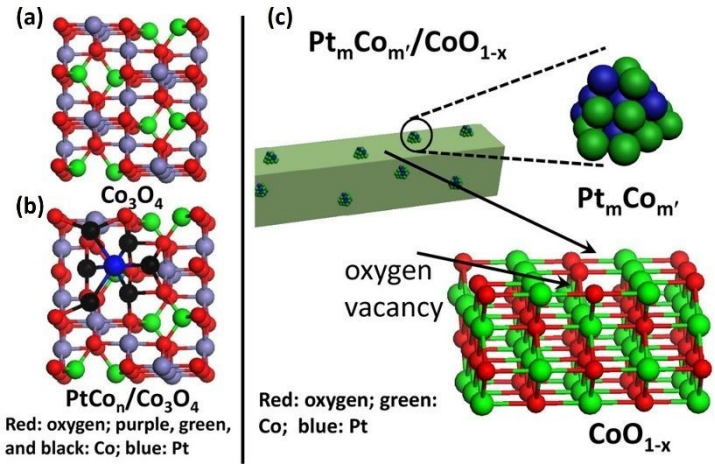

Figure 7 Structural models of surfaces of pure Co_3O_4 and active catalysts, (a) Top view of pure Co_3O_4. (b) Top view of Pt_1Co_n/Co_3O_4. (c) Diagrams of synergistic active sites in $Pt_mCo_{m'}/CoO_{1-x}$.

View Article Online
DOI: 10.1039/D5TA02030A

AUTHOR INFORMATION

Corresponding Author

*Shuangde Li: sdli@ipe.ac.cn

*Yunfa Chen: chenyf@ipe.ac.cn

Authors

Shikun Wang - State Key Laboratory of Mesoscience and Engineering, Institute of Process Engineering, Chinese Academy of Sciences, Beijing 100190, People's Republic of China; University of Chinese Academy of Sciences, No. 19A Yuquan Road, Beijing 100049, People's Republic of China.

Shuangde Li - State Key Laboratory of Mesoscience and Engineering, Institute of Process Engineering, Chinese Academy of Sciences, Beijing 100190, People's Republic of China; University of Chinese Academy of Sciences, No. 19A Yuquan Road, Beijing 100049, People's Republic of China.

Linfeng Nie - State Key Laboratory of Mesoscience and Engineering, Institute of Process Engineering, Chinese Academy of Sciences, Beijing 100190, People's Republic of China.

Yunfa Chen - State Key Laboratory of Mesoscience and Engineering, Institute of Process Engineering, Chinese Academy of Sciences, Beijing 100190, People's

View Article Online
DOI: 10.1039/D5TA02030A

Republic of China; University of Chinese Academy of Sciences, No. 19A Yuquan Road, Beijing 100049, People's Republic of China.

Notes

The authors declare no competing financial interest.

ACKNOWLEDGMENT

This research described above was financially supported by the National Natural Science Foundation of China (NO.22421003) and the Strategic Priority Research Program (A) of the Chinese Academy of Sciences (XDA0390000)..

View Article Online
DOI: 10.1039/D5TA02030A

REFERENCES

(1) Zhou, L.; Liu, Y.; Liu, S.; Zhang, H.; Wu, X.; Shen, R.; Liu, T.; Gao, J.; Sun, K.; Li, B.; et al. For more and purer hydrogen-the progress and challenges in water gas shift reaction. *Journal of Energy Chemistry* **2023**, *83*, 363-396. DOI: 10.1016/j.jechem.2023.03.055.

(2) Zhao, Z.; Ren, H.; Yang, D.; Han, Y.; Shi, J.; An, K.; Chen, Y.; Shi, Y.; Wang, W.; Tan, J.; et al. Boosting nitrogen activation via bimetallic organic frameworks for photocatalytic ammonia synthesis. *ACS Catalysis* **2021**, *11* (15), 9986-9995. DOI: 10.1021/acscatal.1c02465.

(3) Jacobs, G.; Patterson, P. M.; Williams, L.; Chenu, E.; Sparks, D.; Thomas, G.; Davis, B. H. Water-gas shift: In situ spectroscopic studies of noble metal promoted ceria catalysts for CO removal in fuel cell reformers and mechanistic implications. *Applied Catalysis A: General* **2004**, *262* (2), 177-187. DOI: 10.1016/j.apcata.2003.11.025.

(4) Zhang, K.; Guo, Q.; Wang, Y.; Cao, P.; Zhang, J.; Heggen, M.; Mayer, J.; Dunin-Borkowski, R. E.; Wang, F. Ethylene carbonylation to 3-Pentanone with in situ hydrogen via a water-gas shift reaction on Rh/CeO_2. *ACS Catalysis* **2023**, *13* (5), 3164-3169. DOI: 10.1021/acscatal.2c06123.

(5) Ratnasamy, C.; Wagner, J. P. Water gas shift catalysis. *Catalysis Reviews* **2009**, *51* (3), 325-440. DOI: 10.1080/01614940903048661.

View Article Online
DOI: 10.1039/D5TA02030A

593 (6) Newsome, D. S. The water-gas shift reaction. *Catalysis Reviews* **2006**, *21* (2),
594 275-318. DOI: 10.1080/03602458008067535.

595 (7) Lee, D.-W.; Lee, M. S.; Lee, J. Y.; Kim, S.; Eom, H.-J.; Moon, D. J.; Lee, K.-Y.
596 The review of Cr-free Fe-based catalysts for high-temperature water-gas shift reactions.
597 *Catalysis Today* **2013**, *210*, 2-9. DOI: 10.1016/j.cattod.2012.12.012.

598 (8) Baraj, E.; Ciahotný, K.; Hlinčík, T. The water gas shift reaction: Catalysts and
599 reaction mechanism. *Fuel* **2021**, *288*, 119817-119832. DOI:
600 10.1016/j.fuel.2020.119817.

601 (9) Liu, J.; Burciaga, R.; Tang, S.; Ding, S.; Ran, H.; Zhao, W.; Wang, G.; Zhuang,
602 Z.; Xie, L.; Lyu, Z.; et al. Heterogeneous catalysis for the environment. *The Innovation*
603 *Materials* **2024**, *2* (3), 100090. DOI: 10.59717/j.xinn-mater.2024.100090.

604 (10) Meshkani, F.; Rezaei, M. Promoted Fe_2O_3-Al_2O_3-CuO chromium-free catalysts
605 for high-temperature water-gas shift reaction. *Chemical Engineering & Technology*
606 **2015**, *38* (8), 1380-1386. DOI: 10.1002/ceat.201400668.

607 (11) Foppa, L.; Margossian, T.; Kim, S. M.; Muller, C.; Coperet, C.; Larmier, K.;
608 Comas-Vives, A. Contrasting the role of Ni/Al_2O_3 interfaces in water-gas shift and dry
609 reforming of methane. *Journal of the American Chemical Society* **2017**, *139* (47),
610 17128-17139. DOI: 10.1021/jacs.7b08984.

View Article Online
DOI: 10.1039/D5TA02030A

611 (12) Yan, H.; Qin, X.-T.; Yin, Y.; Teng, Y.-F.; Jin, Z.; Jia, C.-J. Promoted Cu-Fe_3O_4
612 catalysts for low-temperature water gas shift reaction: Optimization of Cu content.
613 *Applied Catalysis B: Environmental* **2018**, *226*, 182-193. DOI:
614 10.1016/j.apcatb.2017.12.050.

615 (13) Li, J.; Chen, J.; Song, W.; Liu, J.; Shen, W. Influence of zirconia crystal phase
616 on the catalytic performance of Au/ZrO_2 catalysts for low-temperature water gas shift
617 reaction. *Applied Catalysis A: General* **2008**, *334* (1-2), 321-329. DOI:
618 10.1016/j.apcata.2007.10.020.

619 (14) Jeong, D.-W.; Na, H.-S.; Shim, J.-O.; Jang, W.-J.; Roh, H.-S. A crucial role for
620 the CeO_2-ZrO_2 support for the low temperature water gas shift reaction over Cu-CeO_2-
621 ZrO_2 catalysts. *Catalysis Science & Technology* **2015**, *5* (7), 3706-3713. DOI:
622 10.1039/c5cy00499c.

623 (15) Twigg, M. V.; Spencer, M. S. Deactivation of supported copper metal catalysts
624 for hydrogenation reactions. *Applied Catalysis A: General* **2001**, *212* (1-2), 161-174.
625 DOI: 10.1016/s0926-860x(00)00854-1.

626 (16) Lin, X.; Chen, C.; Ma, J.; Fang, X.; Zhan, Y.; Zheng, Q. Promotion effect of
627 Nb^{5+} for Cu/CeO_2 water-gas shift reaction catalyst by generating mobile electronic
628 carriers. *International Journal of Hydrogen Energy* **2013**, *38* (27), 11847-11852. DOI:
629 10.1016/j.ijhydene.2013.07.001.

View Article Online
DOI: 10.1039/D5TA02030A

630 (17) Jiang, H.; Caro, J. Interfacial Au/MoC catalyst for low-temperature water-gas
631 shift reaction. *Chem* **2017**, *3* (2), 209-210. DOI: 10.1016/j.chempr.2017.07.016.

632 (18) Liu, K.; Li, Y.; Guo, L.; Zhang, Z.; Han, L.; Zheng, D.; Yang, X.; Zhang, Y.;
633 Liao, W. Heralding the electrification era of catalysts: A highly practical current-
634 assisted catalytic strategy. *The Innovation* **2025**, *6* (4). DOI:
635 10.1016/j.xinn.2025.100804.

636 (19) Andreeva, D.; Idakiev, V.; Tabakova, T.; Andreev, A. low-temperature water-
637 gas shift reaction over Au/α-Fe_2O_3. *Journal of Catalysis* **1996**, *158* (1), 354-355. DOI:
638 10.1006/jcat.1996.0035.

639 (20) Sakurai, H.; Ueda, A.; Kobayashi, T.; Haruta, M. Low-temperature water-gas
640 shift reaction over gold deposited on TiO_2. *Chemical Communications* **1997**, (3), 271-
641 272. DOI: 10.1039/a606192c.

642 (21) Chen, Y.; Lin, J.; Wang, X. Noble-metal based single-atom catalysts for the
643 water-gas shift reaction. *Chem Commun (Camb)* **2021**, *58* (2), 208-222. DOI:
644 10.1039/d1cc04051k.

645 (22) Palma, V.; Ruocco, C.; Cortese, M.; Renda, S.; Meloni, E.; Festa, G.; Martino,
646 M. Platinum based catalysts in the water gas shift reaction: Recent advances. *Metals*
647 **2020**, *10* (7). DOI: 10.3390/met10070866.

View Article Online
DOI: 10.1039/D5TA02030A

(23) Qiao, B.; Wang, A.; Yang, X.; Allard, L. F.; Jiang, Z.; Cui, Y.; Liu, J.; Li, J.; Zhang, T. Single-atom catalysis of CO oxidation using Pt_1/FeO_x. *Nature Chemistry* **2011**, *3* (8), 634-641. DOI: 10.1038/nchem.1095.

(24) Zhang, L.; Han, L.; Liu, H.; Liu, X.; Luo, J. Potential-cycling synthesis of single platinum atoms for efficient hydrogen evolution in neutral media. *Angewandte Chemie International Edition in English* **2017**, *56* (44), 13694-13698. DOI: 10.1002/anie.201706921.

(25) Ding, K.; Gulec, A.; Johnson, A. M.; Schweitzer, N. M.; Stucky, G. D.; Marks, L. D.; Stair, P. C. Identification of active sites in CO oxidation and water-gas shift over supported Pt catalysts. *Science* **2015**, *350* (6257), 189-192. DOI: 10.1126/science.aac6368.

(26) Pal, D. B.; Chand, R.; Upadhyay, S. N.; Mishra, P. K. Performance of water gas shift reaction catalysts: A review. *Renewable and Sustainable Energy Reviews* **2018**, *93*, 549-565. DOI: 10.1016/j.rser.2018.05.003.

(27) Lee, Y.-L.; Kim, K.-J.; Hong, G.-R.; Roh, H.-S. Target-oriented water-gas shift reactions with customized reaction conditions and catalysts. *Chemical Engineering Journal* **2023**, *458*. DOI: 10.1016/j.cej.2023.141422.

(28) Taylor, H. S. A theory of the catalytic surface. *Proceedings of the Royal Society of London. Series A, Containing Papers of a Mathematical and Physical Character* **1925**, *108* (745), 105-111. DOI: 10.1098/rspa.1925.0061.

View Article Online
DOI: 10.1039/D5TA02030A

668 (29) Zhu, M.; Wachs, I. E. Iron-based catalysts for the high-temperature water-gas
669 shift (HT-WGS) reaction: A review. *ACS Catalysis* **2015**, *6* (2), 722-732. DOI:
670 10.1021/acscatal.5b02594.

671 (30) Huang, L.; Han, B.; Zhang, Q.; Fan, M.; Cheng, H. Mechanistic study on water
672 gas shift reaction on the Fe_3O_4 (111) reconstructed surface. *The Journal of Physical*
673 *Chemistry C* **2015**, *119* (52), 28934-28945. DOI: 10.1021/acs.jpcc.5b09192.

674 (31) Vecchietti, J.; Bonivardi, A.; Xu, W.; Stacchiola, D.; Delgado, J. J.; Calatayud,
675 M.; Collins, S. E. Understanding the role of oxygen vacancies in the water gas shift
676 reaction on ceria-supported platinum catalysts. *ACS Catalysis* **2014**, *4* (6), 2088-2096.
677 DOI: 10.1021/cs500323u.

678 (32) Yu, K.; Lou, L. L.; Liu, S.; Zhou, W. Asymmetric oxygen vacancies: the intrinsic
679 redox active sites in metal oxide catalysts. *Advanced Science* **2019**, *7* (2). DOI:
680 10.1002/advs.201901970.

681 (33) Lin, X.; Li, R.; Zhang, Y.; Zhan, Y.; Chen, C.; Zheng, Q.; Ma, J. The role of
682 surface copper species in Cu-Fe composite oxide catalysts for the water gas shift
683 reaction. *International Journal of Hydrogen Energy* **2015**, *40* (4), 1735-1741. DOI:
684 10.1016/j.ijhydene.2014.11.105.

685 (34) Andreeva, D.; Idakiev, V.; Tabakova, T.; Andreev, A.; Giovanoli, R. Low-
686 temperature water-gas shift reaction on Au/α-Fe_2O_3 catalyst. *Applied Catalysis A:*
687 *General* **1996**, *134* (2), 275-283. DOI: 10.1016/0926-860x(95)00208-1.

View Article Online
DOI: 10.1039/D5TA02030A

(35) Yang, M.; Allard, L. F.; Flytzani-Stephanopoulos, M. Atomically dispersed Au-$(OH)_x$ species bound on titania catalyze the low-temperature water-gas shift reaction. *Journal of the American Chemical Society* **2013**, *135* (10), 3768-3771. DOI: 10.1021/ja312646d.

(36) Tang, H.; Sun, H.; Chen, D.; Jiao, X. Fabrication of Pt/CeO_2 nanofibers for use in water-gas shift reaction. *Materials Letters* **2012**, *77*, 7-9. DOI: 10.1016/j.matlet.2012.02.122.

(37) Kalamaras, C. M.; Petallidou, K. C.; Efstathiou, A. M. The effect of La^{3+}-doping of CeO_2 support on the water-gas shift reaction mechanism and kinetics over $Pt/Ce_{1-x}La_xO_{2-\delta}$. *Applied Catalysis B: Environmental* **2013**, *136-137*, 225-238. DOI: 10.1016/j.apcatb.2013.02.003.

(38) Petallidou, K. C.; Efstathiou, A. M. Low-temperature water-gas shift on $Pt/Ce_{1-x}La_xO_{2-\delta}$: Effect of Ce/La ratio. *Applied Catalysis B: Environmental* **2013**, *140-141*, 333-347. DOI: 10.1016/j.apcatb.2013.04.007.

(39) Ebrahimi, P.; Kumar, A.; Khraisheh, M. A review of recent advances in water-gas shift catalysis for hydrogen production. *Emergent Materials* **2020**, *3* (6), 881-917. DOI: 10.1007/s42247-020-00116-y.

(40) Yu, K.; Lei, D.; Feng, Y.; Yu, H.; Chang, Y.; Wang, Y.; Liu, Y.; Wang, G.-C.; Lou, L.-L.; Liu, S.; et al. The role of Bi-doping in promoting electron transfer and

View Article Online
DOI: 10.1039/D5TA02030A

707 catalytic performance of Pt/3DOM-$Ce_{1-x}BiO_{2-\delta}$. *Journal of Catalysis* **2018**, *365*, 292-
708 302. DOI: 10.1016/j.jcat.2018.06.025.

709 (41) Liu, N.; Xu, M.; Yang, Y.; Zhang, S.; Zhang, J.; Wang, W.; Zheng, L.; Hong,
710 S.; Wei, M. $Au^{\delta-}$-O_v-Ti^{3+} interfacial site: catalytic active center toward low-temperature
711 water gas shift reaction. *ACS Catalysis* **2019**, *9* (4), 2707-2717. DOI:
712 10.1021/acscatal.8b04913.

713 (42) Xu, M.; He, S.; Chen, H.; Cui, G.; Zheng, L.; Wang, B.; Wei, M. TiO_{2-x}-modified
714 Ni nanocatalyst with tunable metal-support interaction for water-gas shift reaction.
715 *ACS Catalysis* **2017**, *7* (11), 7600-7609. DOI: 10.1021/acscatal.7b01951.

716 (43) Xu, M.; Yao, S.; Rao, D.; Niu, Y.; Liu, N.; Peng, M.; Zhai, P.; Man, Y.; Zheng,
717 L.; Wang, B.; et al. Insights into interfacial synergistic catalysis over Ni@TiO_{2-x} catalyst
718 toward water-gas shift reaction. *Journal of the American Chemical Society* **2018**, *140*
719 (36), 11241-11251. DOI: 10.1021/jacs.8b03117.

720 (44) Li, Y.; Kottwitz, M.; Vincent, J. L.; Enright, M. J.; Liu, Z.; Zhang, L.; Huang,
721 J.; Senanayake, S. D.; Yang, W. D.; Crozier, P. A.; et al. Dynamic structure of active
722 sites in ceria-supported Pt catalysts for the water gas shift reaction. *Nature*
723 *Communication* **2021**, *12* (1), 914. DOI: 10.1038/s41467-021-21132-4.

724 (45) Chen, A.; Yu, X.; Zhou, Y.; Miao, S.; Li, Y.; Kuld, S.; Sehested, J.; Liu, J.; Aoki,
725 T.; Hong, S.; et al. Structure of the catalytically active copper-ceria interfacial
726 perimeter. *Nature Catalysis* **2019**, *2* (4), 334-341. DOI: 10.1038/s41929-019-0226-6.

View Article Online
DOI: 10.1039/D5TA02030A

(46) Lin, L.; Zhou, W.; Gao, R.; Yao, S.; Zhang, X.; Xu, W.; Zheng, S.; Jiang, Z.; Yu, Q.; Li, Y. W.; et al. Low-temperature hydrogen production from water and methanol using Pt/α-MoC catalysts. *Nature* **2017**, *544* (7648), 80-83. DOI: 10.1038/nature21672.

(47) Shao, T.; Cao, L.; Li, L.; Su, Y.; Hou, B.; Lin, J.; Wang, X. A noble-metal-free catalyst with MoC nanorod for low-temperature water gas shift reaction. *Chemical Engineering Journal* **2024**, *485*. DOI: 10.1016/j.cej.2024.149967.

(48) Yao, S.; Zhang, X.; Zhou, W.; Gao, R.; Xu, W.; Ye, Y.; Lin, L.; Wen, X.; Liu, P.; Chen, B.; et al. Atomic-layered Au clusters on α-MoC as catalysts for the low-temperature water-gas shift reaction. *Science* **2017**, *357* (6349), 389-393. DOI: 10.1126/science.aah4321.

(49) Deng, Y.; Ge, Y.; Xu, M.; Yu, Q.; Xiao, D.; Yao, S.; Ma, D. Molybdenum carbide: controlling the geometric and electronic structure of noble metals for the activation of O-H and C-H bonds. *Accounts of Chemical Research* **2019**, *52* (12), 3372-3383. DOI: 10.1021/acs.accounts.9b00182.

(50) Zhang, X.; Zhang, M.; Deng, Y.; Xu, M.; Artiglia, L.; Wen, W.; Gao, R.; Chen, B.; Yao, S.; Zhang, X.; et al. A stable low-temperature H_2-production catalyst by crowding Pt on alpha-MoC. *Nature* **2021**, *589* (7842), 396-401. DOI: 10.1038/s41586-020-03130-6.

View Article Online
DOI: 10.1039/D5TA02030A

746 (51) Rodriguez, J. A.; Ramirez, P. J.; Asara, G. G.; Vines, F.; Evans, J.; Liu, P.; Ricart,
747 J. M.; Illas, F. Charge polarization at a Au-TiC interface and the generation of highly
748 active and selective catalysts for the low-temperature water-gas shift reaction.
749 *Angewandte Chemie International Edition in English* **2014**, *53* (42), 11270-11274.
750 DOI: 10.1002/anie.201407208.

751 (52) Rodriguez, J. A.; Ramírez, P. J.; Gutierrez, R. A. Highly active Pt/MoC and
752 Pt/TiC catalysts for the low-temperature water-gas shift reaction: Effects of the carbide
753 metal/carbon ratio on the catalyst performance. *Catalysis Today* **2017**, *289*, 47-52. DOI:
754 10.1016/j.cattod.2016.09.020.

755 (53) Gnanamani, M. K.; Jacobs, G.; Shafer, W. D.; Sparks, D. E.; Hopps, S.; Thomas,
756 G. A.; Davis, B. H. Low temperature water-gas shift reaction over alkali metal
757 promoted cobalt carbide catalysts. *Topics in Catalysis* **2013**, *57* (6-9), 612-618. DOI:
758 10.1007/s11244-013-0219-7.

759 (54) Babucci, M.; Guntida, A.; Gates, B. C. Atomically dispersed metals on well-
760 defined supports including zeolites and metal-organic frameworks: Structure, bonding,
761 reactivity, and Catalysis. *Chemical Review* **2020**, *120* (21), 11956-11985. DOI:
762 10.1021/acs.chemrev.0c00864.

763 (55) Rivero-Crespo, M. A.; Mon, M.; Ferrando-Soria, J.; Lopes, C. W.; Boronat, M.;
764 Leyva-Perez, A.; Corma, A.; Hernandez-Garrido, J. C.; Lopez-Haro, M.; Calvino, J. J.;
765 et al. Confined Pt_1^{1+} water clusters in a MOF catalyze the low-temperature water-gas

View Article Online
DOI: 10.1039/D5TA02030A

766 shift reaction with both CO_2 oxygen atoms coming from water. *Angewandte Chemie*
767 *International Edition in English* **2018**, *57* (52), 17094-17099. DOI:
768 10.1002/anie.201810251.

769 (56) DeRita, L.; Dai, S.; Lopez-Zepeda, K.; Pham, N.; Graham, G. W.; Pan, X.;
770 Christopher, P. Catalyst architecture for stable single atom dispersion enables site-
771 specific spectroscopic and reactivity measurements of CO adsorbed to Pt atoms,
772 oxidized Pt clusters, and metallic Pt clusters on TiO_2. *Journal of the American Chemical*
773 *Society* **2017**, *139* (40), 14150-14165. DOI: 10.1021/jacs.7b07093.

774 (57) Tepamatr, P.; Charojrochkul, S.; Laosiripojana, N. Water-gas shift activity over
775 Ni/Al_2O_3 composites. *Journal of Composites Science* **2024**, *8* (7). DOI:
776 10.3390/jcs8070239.

777 (58) Lai, X. M.; Xiao, Q.; Ma, C.; Wang, W. W.; Jia, C. J. Heterostructured ceria-
778 titania-supported platinum catalysts for the water gas shift reaction. *ACS Applied*
779 *Materials & Interfaces* **2022**, *14* (6), 8575-8586. DOI: 10.1021/acsami.1c22795.

780 (59) An, J.-W.; Wang, G.-C. Titania crystal-plane-determined activity of copper
781 cluster in water-gas shift reaction. *Applied Surface Science* **2022**, *591*. DOI:
782 10.1016/j.apsusc.2022.153145.

783 (60) Zhao, H.; Yao, S.; Zhang, M.; Huang, F.; Fan, Q.; Zhang, S.; Liu, H.; Ma, D.;
784 Gao, C. Ultra-small platinum nanoparticles encapsulated in sub-50 nm hollow titania

View Article Online
DOI: 10.1039/D5TA02030A

785 nanospheres for low-temperature water-gas shift reaction. *ACS Applied Materials & Interfaces* **2018**, *10* (43), 36954-36960. DOI: 10.1021/acsami.8b12192.

787 (61) Reina, T. R.; Ivanova, S.; Centeno, M. A.; Odriozola, J. A. The role of Au, Cu & CeO_2 and their interactions for an enhanced WGS performance. *Applied Catalysis B: Environmental* **2016**, *187*, 98-107. DOI: 10.1016/j.apcatb.2016.01.031.

790 (62) Fu, X. P.; Guo, L. W.; Wang, W. W.; Ma, C.; Jia, C. J.; Wu, K.; Si, R.; Sun, L. D.; Yan, C. H. Direct identification of active surface species for the water-gas shift reaction on a gold-ceria catalyst. *Journal of the American Chemical Society* **2019**, *141* (11), 4613-4623. DOI: 10.1021/jacs.8b09306.

794 (63) Zhang, L.; Niu, Y.; Pu, Y.; Wang, Y.; Dong, S.; Liu, Y.; Zhang, B.; Liu, Z. W. In situ visualization and mechanistic understandings on facet-dependent atomic redispersion of platinum on CeO_2. *Nano Letter* **2023**, *23* (24), 11999-12005. DOI: 10.1021/acs.nanolett.3c04008.

798 (64) Lin, J.; Wang, A.; Qiao, B.; Liu, X.; Yang, X.; Wang, X.; Liang, J.; Li, J.; Liu, J.; Zhang, T. Remarkable performance of Ir_1/FeO_x single-atom catalyst in water gas shift reaction. *Journal of the American Chemical Society* **2013**, *135* (41), 15314-15317. DOI: 10.1021/ja408574m.

802 (65) Liang, J. X.; Lin, J.; Liu, J.; Wang, X.; Zhang, T.; Li, J. Dual metal active sites in an Ir_1/FeO_x single-atom catalyst: A redox mechanism for the water-gas shift reaction.

804 *Angewandte Chemie International Edition in English* **2020**, *59* (31), 12868-12875.
805 DOI: 10.1002/anie.201914867.

806 (66) Guan, H.; Lin, J.; Qiao, B.; Miao, S.; Wang, A. Q.; Wang, X.; Zhang, T.
807 Enhanced performance of Rh_1/TiO_2 catalyst without methanation in water-gas shift
808 reaction. *AIChE Journal* **2016**, *63* (6), 2081-2088. DOI: 10.1002/aic.15585.

809 (67) Sun, L.; Xu, J.; Liu, X.; Qiao, B.; Li, L.; Ren, Y.; Wan, Q.; Lin, J.; Lin, S.; Wang,
810 X.; et al. High-efficiency water gas shift reaction catalysis on α-MoC promoted by
811 single-atom Ir species. *ACS Catalysis* **2021**, *11* (10), 5942-5950. DOI:
812 10.1021/acscatal.1c00231.

813 (68) Zhang, Z.; Wang, S. S.; Song, R.; Cao, T.; Luo, L.; Chen, X.; Gao, Y.; Lu, J.; Li,
814 W. X.; Huang, W. The most active Cu facet for low-temperature water gas shift
815 reaction. *Nature Communication* **2017**, *8* (1), 488-497. DOI: 10.1038/s41467-017-
816 00620-6.

817 (69) Zhang, Z.; Chen, X.; Kang, J.; Yu, Z.; Tian, J.; Gong, Z.; Jia, A.; You, R.; Qian,
818 K.; He, S.; et al. The active sites of Cu-ZnO catalysts for water gas shift and CO
819 hydrogenation reactions. *Nature Communication* **2021**, *12* (1), 4331. DOI:
820 10.1038/s41467-021-24621-8.

821 (70) Tauster, S. Strong metal-support interactions: Occurrence among the binary
822 oxides of groups IIA-VB. *Journal of Catalysis* **1978**, *55* (1), 29-35. DOI: 10.1016/0021-
823 9517(78)90182-3.

View Article Online
DOI: 10.1039/D5TA02030A

(71) Abdel-Mageed, A. M.; Kučerová, G.; Bansmann, J.; Behm, R. J. Active Au Species During the Low-Temperature Water Gas Shift Reaction on Au/CeO_2: A Time-Resolved Operando XAS and DRIFTS Study. *ACS Catalysis* **2017**, *7*(10), 6471-6484. DOI: 10.1021/acscatal.7b01563.

(72) Jin, C.; Wang, B.; Zhou, Y.; Yang, F.; Han, S.; Guo, P.; Liu, Z.; Shen, W. Gold Atomic Layers and Isolated Atoms on MoC for the Low-Temperature Water Gas Shift Reaction. *ACS Catalysis* **2022**, *12*(24), 15648-15657. DOI: 10.1021/acscatal.2c04651.

(73) Yu, J.; Qin, X.; Yang, Y.; Lv, M.; Yin, P.; Wang, L.; Ren, Z.; Song, B.; Li, Q.; Zheng, L.; et al. Highly Stable Pt/CeO_2 Catalyst with Embedding Structure toward Water-Gas Shift Reaction. *Journal of the American Chemical Society* **2024**, *146*(1), 1071-1080. DOI: 10.1021/jacs.3c12061.

(74) Wang, H.; Hui, Y.; Niu, Y.; He, K.; Vovk, E. I.; Zhou, X.; Yang, Y.; Qin, Y.; Zhang, B.; Song, L.; et al. Construction of $Pt^{\delta+}$-O(H)-Ti^{3+} species for efficient catalytic production of hydrogen. *ACS Catalysis* **2023**, *13*(15), 10500-10510. DOI: 10.1021/acscatal.3c02552.

(75) Tanna, A. R.; Trivedi, U. N.; Chhantbar, M. C.; Joshi, H. H. Influence of Jahn-Teller Cu^{2+}(3d9) ion on structural and magnetic properties of Al-Cr co-substituted $CuFe_2O_4$. *Indian Journal of Physics* **2013**, *87*(11), 1087-1092. DOI: 10.1007/s12648-013-0341-1.

View Article Online
DOI: 10.1039/D5TA02030A

(76) Yin, T.; Meng, F.-Y.; Zhang, M.; Yan, Y.-W. Fabrication and characterization of nanoporous Ag-Pt alloy. *Rare Metals* **2021**, *40* (5), 1203-1207. DOI: 10.1007/s12598-020-01551-w.

(77) Liu, L.; Corma, A. Bimetallic Sites for Catalysis: From Binuclear Metal Sites to Bimetallic Nanoclusters and Nanoparticles. *Chemical Reviews* **2023**, *123* (8), 4855-4933. DOI: 10.1021/acs.chemrev.2c00733.

(78) Chen, G.; Gao, R.; Zhao, Y.; Li, Z.; Waterhouse, G. I. N.; Shi, R.; Zhao, J.; Zhang, M.; Shang, L.; Sheng, G.; et al. Alumina-supported CoFe alloy catalysts derived from layered - double - hydroxide nanosheets for efficient photothermal CO_2 hydrogenation to hydrocarbons. *Advanced Materials* **2017**, *30* (3). DOI: 10.1002/adma.201704663.

(79) Sato, Y.; Terada, K.; Soma, Y.; Miyao, T.; Naito, S. Marked addition effect of Re upon the water gas shift reaction over TiO_2 supported Pt, Pd and Ir catalysts. *Catalysis Communications* **2006**, *7* (2), 91-95. DOI: 10.1016/j.catcom.2005.08.009.

(80) Srichaisiriwech, W.; Tepamatr, P. Monometallic and Bimetallic Catalysts Supported on Praseodymium-Doped Ceria for the Water-Gas Shift Reaction. *Molecules* **2023**, *28* (24), 8146. DOI: 10.3390/molecules28248146.

(81) Jha, A.; Jeong, D.-W.; Shim, J.-O.; Jang, W.-J.; Lee, Y.-L.; Rode, C. V.; Roh, H.-S. Hydrogen production by the water-gas shift reaction using $CuNi/Fe_2O_3$ catalyst. *Catalysis Science & Technology* **2015**, *5* (5), 2752-2760. DOI: 10.1039/c5cy00173k.

View Article Online
DOI: 10.1039/D5TA02030A

863 (82) Zhang, S.; Shan, J. J.; Zhu, Y.; Frenkel, A. I.; Patlolla, A.; Huang, W.; Yoon, S.
864 J.; Wang, L.; Yoshida, H.; Takeda, S.; et al. WGS catalysis and in situ studies of CoO_{1-x},
865 $PtCo_n/Co_3O_4$, and $Pt_mCo_{m'}/CoO_{1-x}$ nanorod catalysts. *Journal of the American*
866 *Chemical Society* **2013**, *135* (22), 8283-8293. DOI: 10.1021/ja401967y.

867 (83) Xia, S.; Fang, L.; Meng, Y.; Zhang, X.; Zhang, L.; Yang, C.; Ni, Z. Water-gas
868 shift reaction catalyzed by layered double hydroxides supported Au-Ni/Cu/Pt bimetallic
869 alloys. *Applied Catalysis B: Environmental* **2020**, *272*. DOI:
870 10.1016/j.apcatb.2020.118949.

871 (84) Yang, M.; Li, S.; Wang, Y.; Herron, J. A.; Xu, Y.; Allard, L. F.; Lee, S.; Huang,
872 J.; Mavrikakis, M.; Flytzani-Stephanopoulos, M. Catalytically active Au-$O(OH)_x$-
873 species stabilized by alkali ions on zeolites and mesoporous oxides. *Science* **2014**, *346*
874 (6216), 1498-1501. DOI: 10.1126/science.1260526.

875 (85) Kaftan, A.; Kusche, M.; Laurin, M.; Wasserscheid, P.; Libuda, J. KOH-promoted
876 Pt/Al_2O_3 catalysts for water gas shift and methanol steam reforming: An operando
877 DRIFTS-MS study. *Applied Catalysis B: Environmental* **2017**, *201*, 169-181. DOI:
878 10.1016/j.apcatb.2016.08.016.

879 (86) Ang, M. L.; Oemar, U.; Saw, E. T.; Mo, L.; Kathiraser, Y.; Chia, B. H.; Kawi,
880 S. Highly active $Ni/xNa/CeO_2$ catalyst for the water-gas shift reaction: Effect of sodium
881 on methane suppression. *ACS Catalysis* **2014**, *4* (9), 3237-3248. DOI:
882 10.1021/cs500915p.

View Article Online
DOI: 10.1039/D5TA02030A

883

884

View Article Online
DOI: 10.1039/D5TA02030A

View Article Online
DOI: 10.1039/D5TA02030A

Data Availability Statement

Dear Editor:

No primary research results, software or code have been included and no new data were generated or analysed as part of this review.

Sincerely,

Professor, Dr. Yunfa Chen

Institute of Process Engineering, Chinese Academy of Sciences

(chenyf@ipe.ac.cn)